

Interpretable Neural Networks with Random Constructive Algorithm

Jing Nan, Wei Dai, *Senior Member, IEEE*

Abstract—This paper introduces an Interpretable Neural Network (INN) incorporating spatial information to tackle the opaque parameterization process of random weighted neural networks. The INN leverages spatial information to elucidate the connection between parameters and network residuals. Furthermore, it devises a geometric relationship strategy using a pool of candidate nodes and established relationships to select node parameters conducive to network convergence. Additionally, a lightweight version of INN tailored for large-scale data modeling tasks is proposed. The paper also showcases the infinite approximation property of INN. Experimental findings on various benchmark datasets and real-world industrial cases demonstrate INN’s superiority over other neural networks of the same type in terms of modeling speed, accuracy, and network structure.

Index Terms—Interpretable neural networks, UAP, data analysis, data modeling.

I. INTRODUCTION

NEURAL networks, are different from traditional model-based methods in that they excel at extracting intrinsic patterns from complex data. Therefore, it is widely used in various research areas [1]–[3]. Among them, Deep Neural Networks (DNNs) and Flat Neural Networks (FNNs) are the most prominent. DNNs achieve end-to-end learning by combining fine-tuning [4], which endows them with superior expressive and generalisation capabilities. However, DNNs are time-consuming to train. Recently, there has been a surge of interest in stochastic weighted neural networks (RWNNs), which are a type of FNN with universal approximation capabilities [5]–[8]. RWNNs are run through a two-step training mode: firstly, randomly assigning the hidden parameters, and then evaluating the output weights through linear equations.

Random Weighted Neural Networks (RWNNs) have proven advantages, but their network structure is still relatively poorly suited for modelling tasks. A network structure that is excessively large may lead to poor generalization, while one that is overly small may result in inadequate learning capacity. Constructive algorithms typically begin with a modest network structure, often just a single hidden node, and gradually expand it by incrementally adding new hidden nodes until the desired performance criteria are achieved [9]. Consequently, these algorithms tend to provide more conservative network structures for modeling tasks [10]. As a result, the constructive variant of RWNNs, IRWNNs, has been effectively employed in various data modeling endeavors [11]–[13].

In the domain of probability theory, the conventional approach of randomly generating hidden parameters may not always suffice for achieving optimal performance in IRWNNs.

This raises a fundamental question: What defines suitable hidden parameters for IRWNNs? Through a thorough algebraic exploration of multidimensional nonlinear functions, researchers [14] have demonstrated that the relationship between input samples and hidden parameters can be aptly characterized by nonlinear weight equations. Moreover, insights from [15] have unveiled the presence of a supervisory mechanism between hidden parameters and input samples, thereby enhancing network performance. Building upon these foundational insights, [16] introduced a constructive algorithm incorporating a supervisory mechanism to effectively allocate hidden parameters within a dynamic interval. Additionally, [17] proposed a methodology for generating hidden parameters by analyzing the range of input samples and activation functions. More recently, [18] introduced RWNNs with compact incremental inequality constraints, referred to as CIRW, aimed at refining the quality of hidden parameters. Despite these advancements, the precise mechanisms through which hidden parameters fulfill their objectives remain largely unexplored. Consequently, visualizing the influence of each hidden parameter on residual error (indicative of network performance) remains a daunting challenge. Currently, enhancing the interpretability of predicted behaviors of NNs is gaining increasing attention and significance in research [19], [20]. Hence, further exploration into interpretable constructive algorithms is deemed crucial and warranted for advancing the field of RWNNs.

This paper introduces an interpretable neural network. The primary contributions are outlined as follows:

- 1) Utilizing the spatial relationship between hidden parameters and network error, this paper devises an interpretable spatial information constraint to guide the assignment of randomized hidden parameters.
- 2) In two implementations of the algorithms, INN and IN+, which utilise different methods of calculating the output weights of the network, a pool of nodes is used to systematically search for hidden parameters, thus improving the quality of the hidden nodes.

Section II provides a brief overview of RWNNs. In section III, we introduce our proposed INN in detail. Section IV presents the experimental evaluation. Finally, Section V concludes the article, summarising the findings and discussing potential future directions.

II. PROBLEM ANALYSIS

A. RWNN and Constructive Algorithms

In RWNN, all hidden parameters are randomly assigned from a predetermined interval and remain fixed throughout

the training process. The evaluation of output weights is accomplished by solving a system of linear equations. The RWNN are expounded as follows.

For $f : R^d \rightarrow R^m$, the RWNNs with L hidden nodes is $f_L = H\beta$, where $H = [g_1(\omega_1^T \cdot x + b_1), \dots, g_L(\omega_L^T \cdot x + b_L)]$, T denotes matrix transpose, x is the input sample, ω_j and b_j are the input weights and biases of the j -th hidden node, respectively. g_j denotes the nonlinear activation function. β are evaluated by $\beta = H^\dagger f_L$, where $\beta = [\beta_1, \beta_2, \dots, \beta_L]^T$.

Constructive algorithms, owing to their incremental construction approach, tend to discover the minimal network structure. Consequently, these algorithms have been adapted to RWNNs, leading to the introduction of IRWNNs. In particular, if an IRWNN with $L - 1$ hidden nodes fails to meet the termination condition, a new hidden node is generated through the following two steps:

1) The input weights and bias are randomly generated from the fixed interval. Then, the output vector g_L , which is determined by $\Delta = \frac{\langle e_{L-1}, g_L \rangle}{\|g_L\|^2}$. f_{L-1} is the output of IRWNNs.

2) β_L is the output weight of the L -th hidden node.

If $e_L = f - f_L$ does not meet the predefined residual error, then a new hidden node should be added until the predefined residual error is reached.

III. INTERPRETABLE NEURAL NETWORK

This section establishes the interpretable spatial information constraint by leveraging the geometric relationship between the network error and the parameters. The universal approximation property of this constraint is ensured by integrating the residual error. Furthermore, a node pool strategy is adopted to acquire hidden parameters that promote convergence. Lastly, two distinct algorithm implementations are introduced: INN and IN+.

A. Interpretable Spatial Information Constraint

Theorem 1: Suppose that $\text{span}(\Gamma)$ is dense in L^2 and $\forall g \in \Gamma, 0 < \|g\| < v$ for some $v \in R$. If g_L is randomly generated under interpretable spatial information constraint

$$\cos\theta_L \geq \gamma_L \langle e_L, e_L \rangle \quad (1)$$

β_L are evaluated by $\beta_L = \frac{\langle e_{L-1}, g_L \rangle}{\|g_L\|^2}$. Then, we have $\lim_{L \rightarrow +\infty} \|e_L\| = 0$.

Proof: It's easy to know that $\|e_L\|$ is monotonically decreasing as $L \rightarrow \infty$.

It follows from Eq. (1) that

$$\begin{aligned} & \|e_L\|^2 - \tau \|e_{L-1}\|^2 \\ &= \sum_{q=1}^m \langle e_{L-1,q} - \beta_{L,q} g_L, e_{L-1,q} - \beta_{L,q} g_L \rangle \\ & \quad - \sum_{q=1}^m \tau \langle e_{L-1,q}, e_{L-1,q} \rangle \\ &= \gamma_L \|e_{L-1}\|^2 - \frac{\langle e_{L-1}, g_L \rangle^2}{\|g_L\|^2} \end{aligned} \quad (2)$$

Then, we have

$$\begin{aligned} & \langle e_L, g_L \rangle \\ &= \langle e_{L-1}, g_L \rangle - \frac{\langle e_{L-1}, g_L \rangle}{\|g_L\|^2} \langle g_L, g_L \rangle \\ &= 0 \end{aligned} \quad (3)$$

Then, we have

$$\begin{aligned} & \sum_{j=1}^{L-1} \beta_j \langle e_{L-1}, g_j \rangle \\ &= \left\langle e_{L-1}, \sum_{j=1}^{L-1} \beta_j g_j \right\rangle \\ &= \|e_{L-1}\|^2 \end{aligned} \quad (4)$$

where f_{L-1} is orthogonal to e_{L-1} . Thus, we have

$$\begin{aligned} & \exists \beta_j \langle e_{L-1}, g_j \rangle \geq \frac{\|e_{L-1}\|^2}{L-1} \\ & \Rightarrow \frac{|\langle e_{L-1}, g_j \rangle|}{\|g_j\|} \geq \frac{\|e_{L-1}\|^2}{(L-1)\beta_j \|g_j\|} \end{aligned} \quad (5)$$

where $\frac{\|e_{L-1}\|^2}{L-1}$ is the average of $\|e_{L-1}\|^2$.

According to the Fig. 1 and Eq. (5), we have

$$\frac{|\langle g_j, e_{L-1} \rangle|}{\|g_j\|} = (\|e_{L-1}\| \cos\theta_{L-1}) \quad (6)$$

Then, we have

$$\cos\theta_L \geq \varphi \|e_L\|^2 \quad (7)$$

To ensure that Equation (9) holds, γ_L is designed as a dynamic value.

$$\varphi \geq \gamma_L \quad (8)$$

It follows from Eq. (1), (3), (8), and (9) that

$$\begin{aligned} & \|e_L\|^2 - \tau \|e_{L-1}\|^2 \\ & \leq \gamma_L \|e_{L-1}\|^2 - \cos^2\theta_{L-1} \\ & \leq 0 \end{aligned} \quad (9)$$

Then, we have that $\lim_{L \rightarrow +\infty} \|e_L\| = 0$.

B. Node Pooling

While the interpretable spatial information constraint guarantees the UAP of the INN, g_L are initially generated randomly in a single step. This approach may not facilitate rapid reduction of the network residual. Consequently, to optimize Eq. (1), the node pool is employed as follows:

$$(\cos^2\theta_L)_{\max} \geq \gamma_L \langle e_{L-1}, e_{L-1} \rangle \quad (10)$$

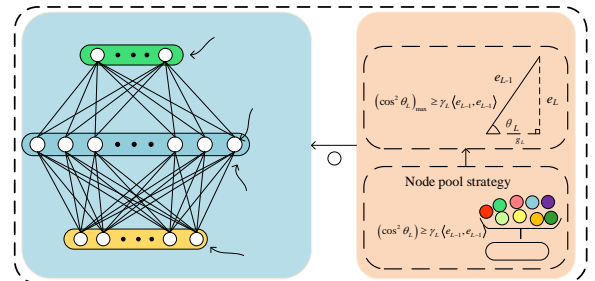


Fig. 1. Network structure of INN.

C. Algorithm steps

Here in this paper, two algorithmic implementations, called INN and IN+, are proposed. Figures 1 and 2 illustrate the network structure and construction process of IC, respectively.

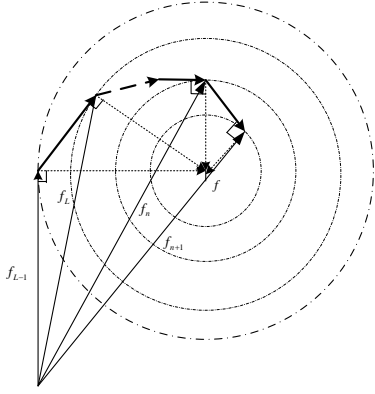


Fig. 2. construction process of INN.

1) *INN*: For a target function $f : R^d \rightarrow R^m$, let's assume that an IC with $L - 1$ hidden nodes has been constructed, i.e., $f_{L-1} = \sum_{j=1}^{L-1} \beta_j g_j(\omega_j^T \cdot x + b_j)$. If the generated g_L makes the interpretable geometric information constraint Eq. (11) hold, and the output weights are given by

$$\beta = H^\dagger f_L \quad (11)$$

Remark 3: Equation 12 is time-consuming when modelling large samples, for this reason we propose a lightweight version, based on Greville theory [21], [22], [23].

2) *IN+*: Let $H_L = [H_{L-1} g_L]$, then, we have that according to Gravel's iteration theory

$$H_L^\dagger = \begin{bmatrix} H_{L-1}^\dagger - d_L b_L^T \\ b_L^T \end{bmatrix} \quad (12)$$

Then, the output weights can be derived as

$$\beta = \begin{bmatrix} \beta^{previous} - d_L b_L^T f \\ b_L^T f \end{bmatrix} \quad (13)$$

IV. EXPERIMENTAL RESULTS

In this section, we present a comparative analysis of the proposed methods: INN, IN+ and other stochastic algorithm comparisons. We leverage six benchmark datasets, one actual mill dataset, and one gesture recognition dataset for our evaluation. The details of these datasets are summarized in Table I. Additionally, Table II provides an overview of each algorithm's information, including experimental parameters used on these datasets.

$$f(x) = \frac{1}{((x - 0.3)^2)} + \frac{1}{((x - 0.9)^2)} - 6 \quad (14)$$

In MATLAB 2020a, the comparison experiments were performed on a personal computer. Each experiment was demonstrated after several repetitions and averaged.

A. Results

1) *Function Approximation Dataset*: Figure 4 depicts the RMSE performance of the four algorithms across the function dataset. It is evident that both the proposed method and CIRW exhibit rapid convergence to the desired RMSE with a minimal number of hidden nodes. Furthermore, both variants of INN

TABLE I
DESCRIPTION OF DATASETS

Data	Test	Train	Various	Label
DB1	400	2000	1	1
DB2	258	2444	561	6
DB3	5330	7200	8	1
DB4	479	1120	15	3
DB5	45	105	4	3
DB6	2947	7563	15	1
DB7	523	1237	1	1

TABLE II
PARAMETERS

Data	IRW		CIR/INN		ℓ	L_{max}
	λ	T_{max}	ζ	T_{max}		
DB1	15		1:1:200	10	0.05	30
DB2	1.5		5:1:50	5	0.05	50
DB3	2	1	1:0.1:3	1	0.05	800
DB4	3		1:1:5	30	0.05	30
DB5	50		1:5:200	15	0.05	10
DB6	0.5		1.5:0.1:7	5	0.05	200
DB7	2		100:10:200	16	0.05	100

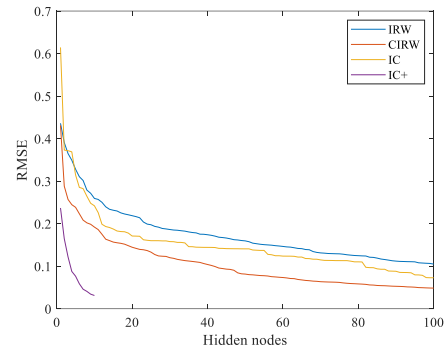


Fig. 3. Convergence of RMSE.

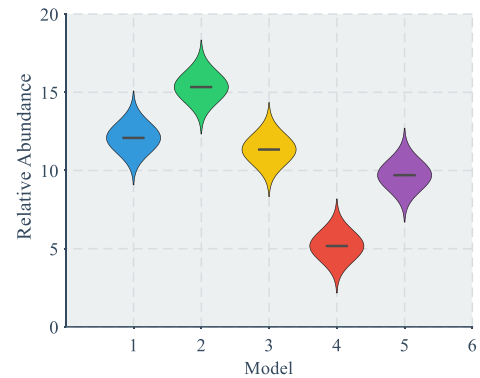


Fig. 4. KDF for four algorithms.

require fewer hidden nodes to achieve the predefined objective, highlighting the compactness advantage of the proposed INN. Transitioning to Figure 5, it presents the KDF of the estimation error. Notably, the KDF of INN closely aligns with the distribution of real data, indicating superior prediction capability compared to other algorithms.

In Figure 6, we explore the impact of different parameters, denoted as λ , on the KDF of IC. Results indicate that varying parameters yield varying effects on the KDF performance of

TABLE III
COMPARISON WITH FOUR ALGORITHMS IN TERMS OF TIME, TRAINING RMSE AND TESTING RMSE ON THE BENCHMARK DATASETS

Dataset	Training time Training RMSE Testing RMSE											
	IRW			CIR			IC			IC+		
Compactiv	0.234s	0.283	0.257	1.215s	0.062	0.071	1.122s	0.062	0.072	0.580s	0.062	0.072
Concrete	0.278s	0.253	0.256	1.09s	0.106	0.206	0.852s	0.095	0.206	0.281s	0.134	0.232
Winequality	0.120s	0.308	0.308	0.314s	0.150	0.159	0.287s	0.150	0.185	0.069s	0.120	0.185
HAR	0.059s	0.160	0.239	0.08s	0.019	0.043	0.080s	0.017	0.042	0.022s	0.028	0.043
ORE	56.401s	0.117	0.149	123.90s	0.016	0.055	123.177s	0.314	0.036	40.259s	0.014	0.038
Segment	0.318s	0.277	0.479	0.590s	0.199	0.218	0.536s	0.194	0.216	0.265s	0.193	0.226

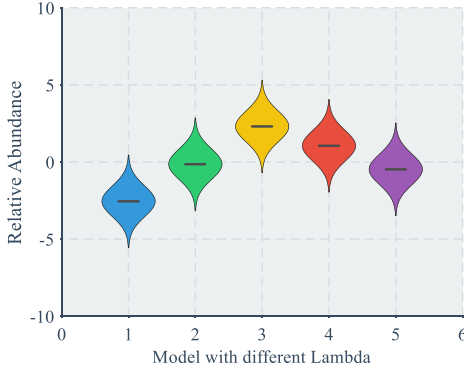


Fig. 5. Impact of λ on KDF.

IC, suggesting that maintaining λ as a fixed value may not optimize KDF performance. This observation underscores the importance of thorough parameter tuning and optimization to achieve optimal model performance and predictive accuracy in the context of IC.

2) *Datasets*: In this section, we delve into the performance analysis of the four algorithms across a spectrum of benchmark datasets. Table III offers insights into the elapsed time and RMSE of these algorithms on the respective datasets. A comprehensive examination of the data in Table III unveils a consistent trend: the training RMSE values of INN consistently outperform those of the other algorithms across all datasets. This consistent superiority suggests that INN possesses the capability to generate higher quality nodes compared to its counterparts. Furthermore, it is noteworthy to highlight that IN+ exhibits weaker performance in comparison. This discrepancy can be attributed to the heavy reliance of IN+ on the quality of the output weights of the initial hidden nodes. The subpar performance of IN+ underscores the importance of carefully considering the initialization strategy and optimization techniques employed in the model, as these factors significantly influence the overall performance and efficacy of the algorithm.

When adding the same number of hidden nodes, it becomes evident that the proposed INN requires less time compared to CIRW. Furthermore, across most datasets, IN+ demonstrates a significant reduction in training time compared to INN, thereby highlighting its superior efficiency. Moving forward to Figure 7, it visually depicts the impact of hidden node pooling on the performance of INN. The experimental findings suggest that both excessively large and excessively small node pools lead to an increase in RMSE. This observation underscores

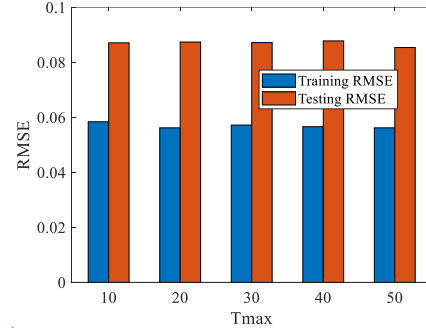


Fig. 6. Impact of node pool on RMSE.

the crucial role of node pool size in influencing the network's efficiency and performance. Therefore, careful consideration of this parameter is imperative during the experimentation process, as highlighted in this study.

B. HGR

HGR finds applications across a spectrum of fields including Augmented Reality (AR), smart home automation, and human health monitoring [24]. In this section, we focus on evaluating the performance of INN within the context of an HGR system. As depicted in Figure 8, the HGR system comprises two essential modules: hardware and software. For our evaluation, we leverage the software component to gather the HGR dataset. This dataset encompasses a total of 2536 samples [25]. Through our analysis, we aim to elucidate the effectiveness and robustness of INN in the realm of hand gesture recognition, shedding light on its potential applications in various domains such as AR, smart home systems, and healthcare monitoring.

Translated with www.DeepL.com/Translator (free version)

1) *Comparison*: Figure 11 displays the Root Mean Square Error (RMSE) of INN in comparison to other methods on HGR. It is noteworthy that INN exhibits remarkable stability in terms of RMSE. Furthermore, the disparity between the maximum and minimum RMSE values of the other algorithms is notably larger, with differences of 0.15 and 0.02, respectively. Table IV provides a comprehensive overview of the experimental outcomes of the four methods applied to HGR. INN demonstrates a clear advantage in both training time and accuracy metrics. Through a thorough comparison and analysis of these results, it becomes evident that the proposed INN outperforms other algorithms in the HGR task, showcasing its efficacy and superiority in this domain.

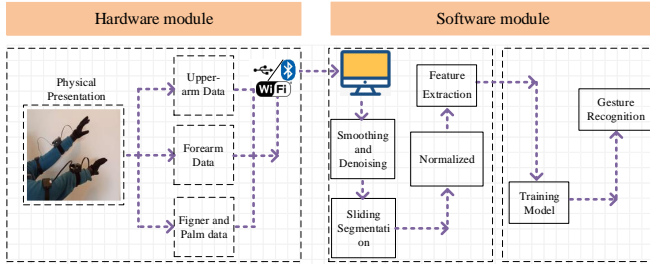


Fig. 7. Framework of HGR.

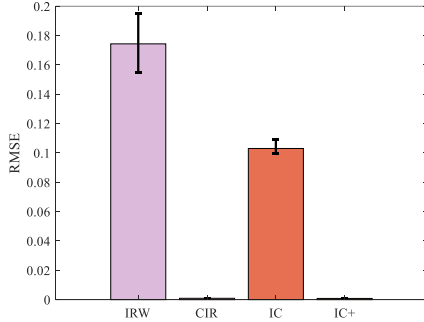


Fig. 8. RMSE of four algorithms.

TABLE IV
PERFORMANCE COMPARISON OF FOUR ALGORITHMS ON HGR

Algorithms	time	Accuracy	Nodes
IRW	20.37s	82.43%	500
CIR	41.63s	95.12%	500
INN	40.79	96.10%	500
IN+	14.68s	96.48%	500

C. ORE

Ore grinding, a crucial step in mineral processing, entails the complete dissociation of valuable ores. The underlying mechanism of ore grinding is highly intricate and multifaceted, rendering the development of a comprehensive mathematical model exceedingly difficult. Consequently, the imperative arises to devise a data-driven model that can proficiently monitor the grinding process. The primary aim of the ore grinding model is to discern and delineate the intricate mapping relationships between various variables involved in the grinding process. By accurately capturing these relationships, the model can provide valuable insights into optimizing the grinding process, enhancing efficiency, and maximizing the extraction of valuable minerals from ores.

$$\text{ORE} = f(B_1, B_2, B_3, A_1, A_2) \quad (15)$$

1) *Discussion*: Figure 14 illustrates the error Probability Density Functions (PDFs) of INN alongside its comparison methods. Notably, INN and IN+ exhibit a similar PDF curve owing to their comparable performance. It is evident that both INN and IN+ surpass the other methods as their curves closely resemble the normal distribution compared to alternative algorithms. This observation underscores IN's superior performance in Outlier Recognition and Elimination (ORE). Table V presents the experimental outcomes of the four methods

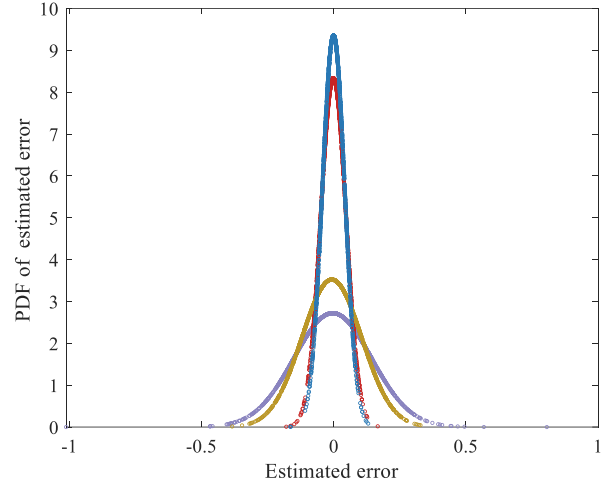


Fig. 9. PDF of all algorithms.

TABLE V
PERFORMANCE COMPARISON OF FOUR ALGORITHMS ON ORE

Algorithms	Training time	Accuracy	Nodes
IRW	0.57s	85.89%	100
CIR	3.93s	95.53%	100
INN	3.29s	95.67%	100
IN+	1.91s	95.81%	100

applied to ORE. Despite INN's prolonged training duration, it excels in terms of accuracy. Through the experimental results and analysis, the proposed algorithm demonstrates commendable performance in terms of generalization and training time.

V. CONCLUSION

IN+ is a further extension of Interpretable Neural Networks (INN), aimed at enhancing both efficiency and performance. Unlike traditional INN, IN+ introduces new features and techniques to further optimize the network's behavior. Firstly, IN+ offers a more efficient method for generating nodes. Instead of the spatially constrained random node generation used in INN, IN+ employs smarter algorithms or optimization strategies to select and arrange nodes, thereby improving the training and inference efficiency of the network. Secondly, IN+ introduces more refined techniques for analyzing node influences. In addition to intuitively demonstrating the impact of each hidden node on network error, IN+ further analyzes the interactions and influences between nodes to provide a more comprehensive and detailed explanation. Furthermore, IN+ may include customized optimizations tailored to specific tasks or datasets. By conducting in-depth analyses of the requirements of different tasks and adjusting the network structure, parameters, or algorithms accordingly, IN+ can achieve better performance. Finally, extensive experiments on various public and real-world datasets have been conducted to validate IN+. The experimental results demonstrate that compared to traditional INN or other methods, IN+ not only reduces computational overhead but also further enhances network performance and behavior. Overall, IN+ represents

a significant advancement in the field of interpretable neural networks. It not only provides more effective explanatory capabilities but also achieves significant improvements in performance and efficiency, opening up new directions for the development of interpretable artificial intelligence.

REFERENCES

- [1] F. Curreri, S. Graziani and M.-G. Xibilia, "Input selection methods for data-driven Soft sensors design: Application to an industrial process," in *Information Sciences.*, vol. 537, pp. 1–17, 2020.
- [2] X.-D. Shi, Q. Kang, H.-Q. Bao, W.-Y. Huang and J. An, "Principal component-based semi-supervised extreme learning machine for soft sensing," in *IEEE Transactions on Automation Science and Engineering.*, doi: 10.1109/TASE.2023.3290352.
- [3] N. Yassaie, S. Gargoum and A.-W. Al-Dabbagh, "Data-Driven Fault Classification in Large-Scale Industrial Processes Using Reduced Number of Process Variables," in *IEEE Transactions on Automation Science and Engineering.*, doi: 10.1109/TASE.2023.3317978.
- [4] P. Zhou, S. Zhang, L. Wen, J. Fu, T.-Y. Chai and H. Wang, "Kalman filter-based data-driven robust model-free adaptive predictive control of a complicated industrial process," in *IEEE Transactions on Automation Science and Engineering.*, vol. 19, pp. 788–803, 2022.
- [5] I.-Y. Tyukin, D.-V. Prokhorov, "Feasibility of random basis function approximators for modeling and control," in *2009 IEEE Control Applications, (CCA) & Intelligent Control, (ISIC), Petersburg.*, pp.1391–1396, 2009.
- [6] Y.-H. Pao and Y. Takefuji, "Functional-link net computing: theory, system architecture, and functionalities," in *Computer.*, vol. 25, pp. 76–79, 1992.
- [7] Y.-H. Pao, G.-H. Park, D.-J. Sobajic, "Learning and generalization characteristics of the random vector Functional-link net," in *Neurocomputing.*, vol. 6, pp. 163–180, 1994.
- [8] B. Igel'nik and Y.-H. Pao, "Stochastic choice of basis functions in adaptive function approximation and the functional-link net," in *IEEE Transactions on Neural Networks.*, vol. 6, pp. 1320–1329, 1995.
- [9] F. Han, J. Jiang, Q. H. Ling, and B. Y. Su, "Stochastic choice of basis functions in adaptive function approximation and the functional-link net," in *Neurocomputing.*, vol. 335, pp. 261–273, 2019.
- [10] X. Wu, P. Rozycki and B. M. Wilamowski, "A hybrid constructive algorithm for single-layer feedforward networks learning," in *IEEE Transactions on Neural Networks and Learning Systems.*, vol. 26, pp. 1659–1668, 2015.
- [11] L.-Y. Ma and K. Khorasani, "Insights into randomized algorithms for neural networks: PractINN issues and common pitfalls," in *IEEE Transactions on Neural Networks and Learning Systems.*, vol. 16, pp. 821–833, 2005.
- [12] J.-X. Peng, K. Li, G.-W. Irwin, "A New Jacobian Matrix for Optimal Learning of Single-Layer Neural Networks," in *IEEE Transactions on Neural Networks.*, vol. 19, pp. 119–129, 2018.
- [13] Dudek G, "A constructive approach to data-driven randomized learning for feedforward neural networks," in *Applied Soft Computing.*, vol. 112, pp. 107797, 2021.
- [14] S. Ferrari and R.-F. Stengel, "Smooth function approximation using neural networks," in *IEEE Transactions on Neural Networks.*, vol. 16, pp. 24–38, 2005.
- [15] I.-Y. Tyukin and D.-V. Prokhorov, "Feasibility of random basis function approximators for modeling and control," in *2009 IEEE Control Applications, (CCA) & Intelligent Control.*, 2009, pp. 1391–1396.
- [16] D.-H. Wang and M. Li, "Stochastic configuration networks: fundamentals and algorithms," in *IEEE Transactions on Cybernetics.*, vol. 47, pp. 3466–3479, 2017.
- [17] G. Dudek, "Generating random weights and biases in feedforward neural networks with random hidden nodes," in *Information Sciences.*, vol. 481, pp. 33–56, 2019.
- [18] Q.-J. Wang, W. Dai, "Compact incremental random weight network for estimating the underground airflow quantity," in *IEEE Transactions on Industrial Informatics.*, vol. 13, pp. 426–436, 2022.
- [19] M. Islam, D.-T. Anderson, A.-J. Pinar, T.-C. Havens, G. Scott and J.-M. Keller, "Enabling explainable fusion in deep learning with fuzzy integral neural networks," in *IEEE Transactions on Fuzzy Systems.*, vol. 28, pp. 1291–1300, 2020.
- [20] H. Sasaki, Y. Hidaka and H. Igarashi, "Explainable deep neural network for design of electric motors," in *IEEE Transactions on Magnetics.*, vol. 57, pp. 1–4, 2021.
- [21] C.-L.-P. Chen and Z.-L. Liu, "Broad learning system: An effective and efficient incremental learning system without the need for deep architecture," in *IEEE Transactions on Neural Networks and Learning Systems.*, vol. 29, pp. 10–24, 2018.
- [22] S.-L. Issa, Q.-M. Peng and X.-G. You, "Emotion classification using EEG brain signals and the broad learning system," in *IEEE Transactions on Systems, Man, and Cybernetics: Systems.*, vol. 51, pp. 7382–7391, 2021.
- [23] L. Cheng, Y. Liu, Z.-G. Hou, M. Tan, D. Du and M. Fei, "A rapid spiking neural network approach with an applNN on hand gesture recognition," in *IEEE Transactions on Cognitive and Developmental Systems.*, vol. 13, pp. 151–161, 2021.
- [24] H. Cheng, L. Yang and Z. Liu, "Survey on 3D hand gesture recognition," in *IEEE Transactions on Circuits and Systems for Video Technology.*, vol. 26, pp. 1659–1673, 2016.
- [25] G. Yuan, X. Liu, Q. Yan, S. Qiao, Z. Wang and L. Yuan, "Hand gesture recognition using deep feature fusion network based on wearable sensors," in *IEEE Sensors Journal.*, vol. 21, pp. 539–547, 2021.
- [26] W. Dai, X.-Y. Zhou, D.-P. Li, S. Zhu and X.-S. Wang, "Hybrid parallel stochastic configuration networks for industrial data analytics," in *IEEE Transactions on Industrial Informatics.*, vol. 18, pp. 2331–2341, 2022.